

Charge, Polarizability, and Photoionization of Single Semiconductor Nanocrystals

Todd D. Krauss and Louis E. Brus

Department of Chemistry, Columbia University, New York, New York 10027

(Received 23 July 1999)

The electrostatic properties of individual CdSe nanocrystals are directly measured using electrostatic force microscopy (EFM) in dry air at room temperature. We determine that the static dielectric constant of CdSe nanocrystals with diameters ~ 5 nm is uniform. However, the charge per nanocrystal is nonuniform, with some nanocrystals possessing a positive charge. Furthermore, a small fraction of the nanocrystals exhibit a blinking behavior in their charge. This is entirely unexpected for a dielectric particle with no additional charge carriers. In addition, EFM measurements with simultaneous photoexcitation provide direct evidence of nanocrystal photoionization and increased blinking behavior.

PACS numbers: 73.61.Tm, 61.16.Ch, 61.46.+w, 73.20.Dx

Semiconductor nanocrystals have attracted much attention over the last decade due to their unique physical properties and potential use for a wide range of applications. (For a recent review, see Refs. [1,2].) In contrast to the optical, electronic, and vibrational properties, the electrostatic properties of semiconductor nanocrystals have received little attention despite their importance. For example, the presence of charge, or electric fields, inside a nanocrystal will significantly affect oscillator strengths, charge carrier lifetimes, electron-phonon coupling, and electron transport properties such as nanocrystal capacitance. These properties need to be understood at room temperature, for they will determine whether semiconductor nanocrystals can eventually be used as new optoelectronic materials, or as quantum devices.

The photoluminescence of single-CdSe nanocrystals demonstrates a fascinating blinking, or "on-off," behavior [3,4]. Similar photoluminescence intermittency phenomena have subsequently been observed for nanocrystals of other materials [5,6]. The photoluminescence blinking was tentatively attributed to a photoionization and subsequent neutralization of the nanocrystal [3]. Direct measurements of the electrostatic charge per nanocrystal during photoexcitation provide a unique method to test this hypothesis.

CdSe crystallizes in the wurtzite structure, which contains a structural dipole moment along the c axis. Thus, in the simplest picture, CdSe nanocrystals should contain a permanent electrostatic polarization, which scales with nanocrystal volume. However, recent theoretical treatments have predicted the presence of a dipole which depends sensitively on surface reconstruction and stoichiometry, rather than only the nanocrystal radius [7]. Therefore, it is important to measure dipole moments of CdSe quantum dots individually.

In previous ensemble studies of CdSe nanocrystals, the presence of an internal electrostatic polarization, resulting from a charge and/or dipole, has been either indirectly measured or inferred. Screened dipole moments, which scaled in magnitude with nanocrystal size, were deter-

mined from dielectric dispersion measurements [8]. Investigations of exciton-phonon coupling [9], two-photon fluorescence excitation [10], and Raman depolarization [11] also suggest a permanent electrostatic polarization in CdSe nanocrystals. Finally, the presence of permanent, internal electric fields in individual CdSe nanocrystals was implied from quantum-confined Stark effect measurements [12].

Here we present direct measurements of the static dielectric constant and electrostatic charge of single semiconductor nanocrystals with and without photoexcitation. CdSe nanocrystals ~ 5 nm in diameter were studied with electrostatic force microscopy (EFM) in dry air at 300 K. We find the dielectric constant of individual CdSe nanocrystals is uniform ($\epsilon \sim 8$). However, the charge per nanocrystal is nonuniform; half of the nanocrystals are neutral and half have a positive charge. Extended photoionization creates additional positive charge on most nanocrystals. This is the first direct measurement of photoionization of individual semiconductor nanocrystals.

Martin, Williams, and Wickramasinghe first demonstrated the remarkable ability of an oscillating atomic force microscope (AFM) tip to measure weak electric fields above a substrate, as a function of lateral position [13]. For small vibrational amplitudes, the electrostatic force on the tip is approximated as a simple-harmonic-type interaction. Thus, the electrostatic force gradient normal to the substrate surface acts as an effective spring constant, which slightly shifts the resonance frequency of the cantilever. Relative changes in the cantilever resonance frequency $\Delta\nu/\nu$ about 1×10^{-5} can be measured, corresponding to electric field strengths from a charge with magnitude of less than one-tenth of an electron.

In EFM measurements, a conductive AFM tip is electrically connected to a conductive substrate. The forces on the AFM tip are given by capacitive and Coulombic terms [14,15]. We model the Coulombic forces assuming any surface charge Q acts as a point charge located directly on the sample surface and generates an image charge in the metal substrate. The charge Q and its image interact with

charges on the AFM tip, including induced charge due to Q . The application of a sinusoidal voltage to the AFM tip, $V = V_{dc} + V_{ac} \sin(\omega t)$, yields components of the force at ω and 2ω , respectively:

$$F(\omega) = \left(\frac{\partial C}{\partial z} (V_{dc} + \phi) + \frac{QC}{4\pi\epsilon_0 z^2} + \frac{Q_1 C}{4\pi\epsilon_0 (z + \frac{2h}{\epsilon_1})^2} + \frac{\partial C}{\partial z} \frac{Q_2}{C} \right) V_{ac}, \quad (1)$$

and

$$F(2\omega) = \frac{\partial C}{\partial z} \frac{V_{ac}^2}{4}. \quad (2)$$

In the above equations, C is the tip-substrate capacitance, ϕ is the contact potential, and z is the separation between the tip and sample surface. Our samples consist of nanocrystals on an insulator with thickness h and dielectric constant ϵ_1 , on a metallic substrate. Q_1 and Q_2 are the induced charges on the metallic substrate and AFM tip, respectively, due to Q . Q_1 and Q_2 are functions of z and h , and are calculated assuming a parallel plate geometry for the tip and substrate. The last term in Eq. (1) represents the force (at ω) from the induced charge Q_2 on the tip. By varying V_{dc} with respect to ϕ , we determine Q from the measured force gradient on the tip at ω [14,15]. Local dielectric properties, which affect dC/dz , are determined by fitting the measured component of the force gradient at 2ω [14].

These equations allow us to understand the changes in cantilever resonance frequency $\Delta\nu(\omega)$ and $\Delta\nu(2\omega)$ as the AFM tip passes over a CdSe nanocrystal. For $\Delta\nu(2\omega)$ (dielectric image), we expect an increase in absolute magnitude when over a nanocrystal due to the larger dielectric constant of CdSe compared to the surrounding air. For $\Delta\nu(\omega)$ (charge image), with V_{dc} set such that $V_{dc} + \phi = 0$, we expect to see one of three types of behavior: a decrease or increase in cantilever resonant frequency corresponding to, respectively, a positively or negatively charged nanocrystal, or $\Delta\nu(\omega) = 0$ for a neutral nanocrystal.

Dilute hexane solutions containing ~ 5 nm diameter, trioctylphosphine oxide (TOPO) capped CdSe nanocrystals (see Ref. [16]), were spun onto a 1–2 nm thick insulator layer on a metallic substrate. Insulator-metal substrates consisted of SiO_2 on Si, a dodecanethiol SAM on Au, and poly(vinyl butyral) (PVB) on highly oriented pyrolytic graphite (HOPG). Images were obtained in a dry box with $< 3\%$ relative humidity. Use of the dry box was necessary to avoid screening by physisorbed water on the sample surface. To image a field of nanocrystals, first a line scan of the sample height was recorded with $V = 0$. The tip was then withdrawn from the surface, the voltage V was applied, and the components of the electrostatic force gradient at ω and 2ω were simultaneously acquired for the same line scan. For photoexcita-

tion measurements, continuous wave light from a HeCd laser ($\lambda = 442$ nm) or a diode laser ($\lambda = 780$ nm) was coupled into a glove box through an optical fiber and focused at grazing incidence onto the sample.

A typical set of EFM images without laser irradiation is shown in Fig. 1. Except for variations due to slight differences in substrate roughness and particle diameter, $\Delta\nu(2\omega)$ is uniform for all nanocrystals, as shown in Fig. 1(c). However, $\Delta\nu(\omega)$ is highly nonuniform among nanocrystals. Approximately half of the nanocrystals have $\Delta\nu(\omega)/\nu \sim -1 \times 10^{-4}$, corresponding to about one positive charge (see discussion below). The other half have no detectable signal, and thus are effectively neutral, as expected for a dielectric particle. Quite unexpectedly, the positive charge of $\sim 1\%$ of the nanocrystals exhibits a blinking, or intermittent behavior, as shown in Fig. 2. The positive charge signal present in the upper portion of Fig. 2(a) vanishes during the lower portion of the scan. No change occurs in the simultaneous dielectric image [Fig. 2(b)]. The time scale for the on-off behavior ranges from seconds to minutes, and the signal magnitude from one “on” period to another is approximately the same. Systematic studies of this on-off behavior are presently being carried out.

Absolute magnitudes for the dielectric constant and surface charge inferred from the raw data depend strongly on the capacitance of the tip-substrate system, and its derivatives with respect to z , which are extremely sensitive to tip geometry. To increase accuracy in these values, we chose to measure the tip-substrate capacitance, without the presence of nanocrystals, directly using EFM. The second derivative of the capacitance follows a power law dependence $d^2C/dz^2 \sim z^{-1.4}$. This implies that the tip-substrate capacitance lies between a sphere-plane ($d^2C/dz^2 \sim z^{-2}$) and a cone-plane ($d^2C/dz^2 \sim z^{-1}$) geometry [17], which is reasonable for a square-pyramidal AFM tip.

The magnitude of the charge per nanocrystal is obtained by fitting Eq. (1) as a function of V_{dc} . With $V_{dc} + \phi \sim 0.05$ V, we find that $\Delta\nu(\omega)$ over a charged nanocrystal vanishes, and this corresponds to $Q \sim 0.1e$, at $h = 1.5$ nm. The accuracy of this value is limited by our accuracy in determining $C(z)$, and also by the neglect of the nanocrystal size and shielding in the model. Since the observed blinking behavior in the charge contains nominally only one on value, we assign the observed positive charge to a screened elementary charge on a nanocrystal. Possible explanations for the origin of this charge include carrier trapping at the nanocrystal surface or a small amount of charged contaminants from the preparation, such as Na^+ . Also, based on the rms noise in the charge image, the nanocrystals which appear “neutral” must contain less than one-tenth of an elementary charge.

Permanent nanocrystal dipole moments, if present, would contribute to the $\Delta\nu(\omega)$ signal. Measurements as a function of tip-substrate separation could distinguish

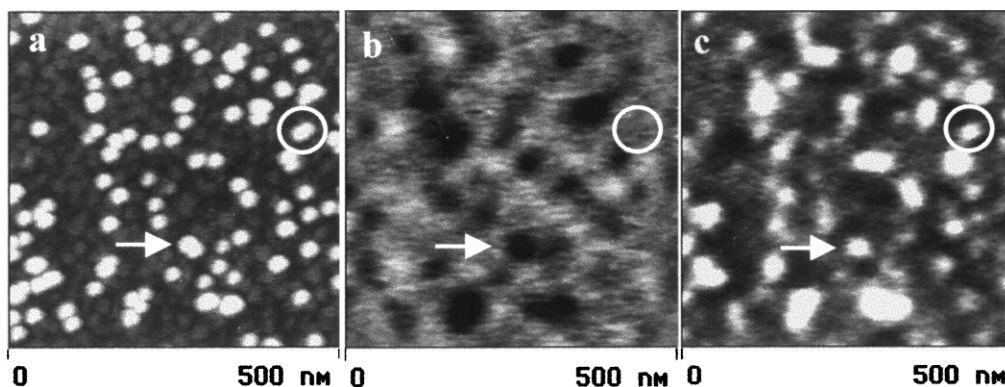


FIG. 1. EFM image of CdSe nanocrystals on 0.1% PVB spun coat from toluene, on a fresh surface of HOPG. (a) Tapping mode AFM height image. Because of the finite end radius of the AFM tip the apparent nanocrystal diameter obtained from height images is artificially enlarged compared with the actual diameter. The EFM images in (b) and (c) correspond to the change in cantilever resonant frequency, $\Delta\nu$, at ω , and 2ω , respectively. They were recorded with a Digital Instruments Nanoscope IIIa operating in linear lift-mode using Digital Instruments SESP or MESP cantilevers with the following parameters: $V_{ac} = 6$ V peak to peak, $\omega = 2\pi \times 800$ Hz, tip-substrate separation ~ 10 nm, and $V_{dc} = -\phi$ (typically $|V_{dc}| < 0.5$ V). The arrow and circle correspond to positively charged and neutral nanocrystals, respectively.

between dipole and charge fields. However, we currently do not have enough dynamic range to make these measurements. Nevertheless, we do not attribute the observed signal to dipole terms because, for a variety of insulators and substrates: (i) the observed charge signal is always zero or positive with one specific value and (ii) the charge signal blinks as might be expected for a thermally induced charge transfer process. With randomly oriented dipoles, a range of positive and negative signals would be expected.

Photoexcitation above the band gap causes many CdSe nanocrystals to increase their positive charge by one unit, $\Delta\nu(\omega)/\nu \sim -1 \times 10^{-4}$, as shown in Fig. 3. Photoionization of individual nanocrystals is not instantaneous but grows in with a time constant of minutes. After laser cutoff, the photoinduced positive charge decays back to the unexcited value with a time constant of hours. Also, photoexcitation increases the number of nanocrystals which

show a blinking behavior of the charge. Photoionization is most probable on samples with thin insulator layers (for example, a dodecanethiol SAM on Au), while the sample with the largest insulator layer (~ 5 nm SiO_2 on Si), shows no evidence of photoionization. Excitation at 780 nm does not affect the EFM signal, and photoexcitation, regardless of laser frequency, does not affect the dielectric image. The fact that the charge signal generated in photoionization is the same magnitude as the signal observed for some nanocrystals without laser irradiation supports the assignment of both signals to one positive charge.

We suggest that upon photoexcitation, the electron has a small probability of tunneling into the metal substrate through the insulator layer. In a CdSe nanocrystal the electron is far more delocalized than the hole, with a non-negligible fraction of the electron density outside the nanocrystal [18]. Thus, when the electron is excited it can possibly escape, resulting in a positively charged nanocrystal. Since the photoexcitation rate is $\sim 10^4$ Hz, the net photoionization probability is $\leq 10^{-5}$ per excitation.

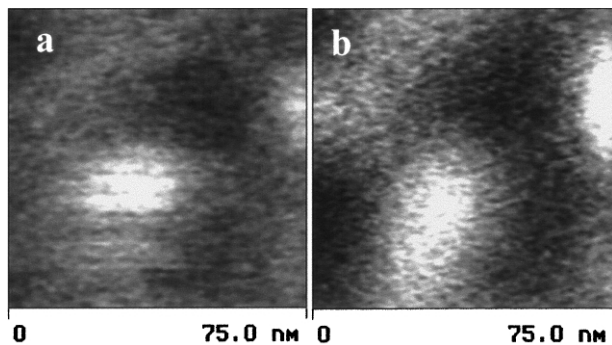


FIG. 2. EFM (a) charge [$\Delta\nu(\omega)$] and (b) dielectric [$\Delta\nu(2\omega)$] image showing blinking behavior of an individual CdSe nanocrystal. The slightly elliptical shape of the nanocrystal is due to piezoelectric scanner drift during the acquisition of the image. The sign of $\Delta\nu(\omega)$ is inverted for clarity.

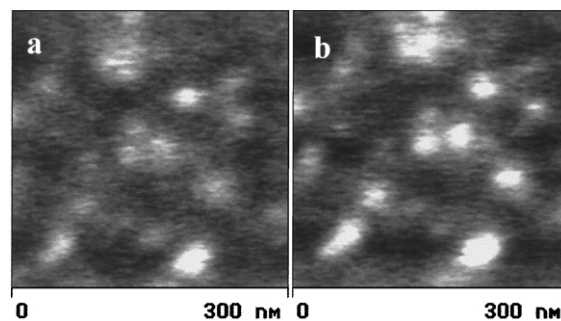


FIG. 3. Charge image recorded as in Fig. 1 before (a) and during (b) excitation at 442 nm. The sign of $\Delta\nu(\omega)$ is inverted for clarity. The laser intensity was ~ 20 W/cm² at the sample.

After the illumination is extinguished, an electron from the metal will tunnel back into the nanocrystal, recombine with the hole, and neutralize the photoinduced charge. Note that laser light at 780 nm, which is less than the CdSe nanocrystal band gap, did not cause photoionization. This implies that photoexcitation in the nanocrystal, and not the metallic substrate, causes the observed net charge. Finally, our results are consistent with current understanding of the electron transport properties of photovoltaic devices made from layers of CdSe nanocrystals [19–22].

This elementary tunneling proposal for explaining the photoionization of individual nanocrystals must be tested by further experiments. However, it is clear that photoexcitation can lead to ionization of the nanocrystal, and an on-off blinking of charge on a time scale of seconds to hours. In the dark the photoinduced charge decays away over time. These observations directly support the photoionization mechanism [3,4] used to explain the nanocrystal photoluminescence blinking.

Over a nanocrystal, the magnitude of the force gradient at 2ω depends on the dielectric constant of a CdSe nanocrystal through the dC/dz term in Eq. (2). Also, the relationship between the force gradient at 2ω , and $\Delta\nu(2\omega)$, depends linearly on the cantilever spring constant [13]. We obtain approximate values for the spring constant by calibrating the measured force gradient on the tip at ω with calculated values. By subsequently fitting Eq. (2), we infer an absolute value of $\epsilon \sim 8$ for a single CdSe nanocrystal. Within experimental uncertainty, this value agrees with the predicted magnitude of the static dielectric constant of 5 nm CdSe nanocrystals, $\epsilon \sim 8.9$ [23]. Also, we find that the thermal and photoinduced positive charge on a single nanocrystal is not polarizable, as the dielectric image does not change in the presence of any charge.

In conclusion, we have examined the dielectric constant and electrostatic polarization of single CdSe nanocrystals. Using EFM, we determine that the static dielectric constant of CdSe nanocrystals is uniform and agrees with the predicted value. However, the charge of individual nanocrystals is nonuniform with a significant fraction of the nanocrystals possessing a positive elementary charge. Photoexcitation with light of frequencies greater than the band gap of the nanocrystals results in slow photoionization and the acquisition of a definite positive charge. The photoinduced positive charge, and its subsequent decay, is consistent with tunneling of the photoexcited electron through the thin insulator and into the metal substrate.

The authors thank Zhonghua Yu and Guanglu Ge for assistance with nanocrystal synthesis and sample

preparation, and Professor George Flynn for the loan of equipment. We also acknowledge the support of the W. M. Keck Foundation in the purchase of the AFM and Bell Laboratories for equipment donation. This research was supported under NSF MRSEC Grant No. DMR-98-09687 for materials research at Columbia University.

-
- [1] A. D. Yoffe, *Adv. Phys.* **42**, 173 (1993).
 - [2] A. P. Alivisatos, *J. Phys. Chem.* **100**, 13 226 (1996).
 - [3] M. Nirmal, B. O. Dabbousi, M. G. Bawendi, J. J. Macklin, J. K. Trautman, T. D. Harris, and L. E. Brus, *Nature (London)* **383**, 802 (1996).
 - [4] M. Nirmal and L. Brus, *Acc. Chem. Res.* **32**, 407 (1999).
 - [5] M. D. Mason, G. M. Credo, K. D. Weston, and S. K. Buratto, *Phys. Rev. Lett.* **80**, 5405 (1998).
 - [6] M.-E. Pistol, P. Castrillo, D. Hessman, J. A. Prieto, and L. Samuelson, *Phys. Rev. B* **59**, 10 725 (1999).
 - [7] E. Rabani, B. Hetényi, B. J. Berne, and L. E. Brus, *J. Chem. Phys.* **110**, 5355 (1999).
 - [8] S. A. Blanton, R. Leheny, M. A. Hines, and P. Guyot-Sionnest, *Phys. Rev. Lett.* **79**, 865 (1997).
 - [9] S. Nomura and T. Kobayashi, *Phys. Rev. B* **45**, 1305 (1992).
 - [10] M. E. Schmidt, S. A. Blanton, M. A. Hines, and P. Guyot-Sionnest, *J. Chem. Phys.* **106**, 5254 (1997).
 - [11] J. J. Shiang, A. V. Kadavanich, R. K. Grubbs, and A. P. Alivisatos, *J. Phys. Chem.* **99**, 17 417 (1995).
 - [12] S. A. Empedocles and M. G. Bawendi, *Science* **278**, 2114 (1997).
 - [13] Y. Martin, C. C. Williams, and H. K. Wickramasinghe, *J. Appl. Phys.* **61**, 4723 (1987).
 - [14] Y. Martin, D. W. Abraham, and H. K. Wickramasinghe, *Appl. Phys. Lett.* **52**, 1103 (1988).
 - [15] B. D. Terris, J. E. Stern, D. Rugar, and H. J. Mamin, *Phys. Rev. Lett.* **63**, 2669 (1989).
 - [16] C. B. Murray, D. J. Norris, and M. G. Bawendi, *J. Am. Chem. Soc.* **115**, 8706 (1993).
 - [17] S. Belaidi, P. Girard, and G. Leveque, *J. Appl. Phys.* **81**, 1023 (1997).
 - [18] D. Schooss, A. Mews, A. Eychmüller, and H. Weller, *Phys. Rev. B* **49**, 17 072 (1994).
 - [19] S.-H. Kim, G. Markovich, S. Rezvani, S. H. Choi, K. L. Wang, and J. R. Heath, *Appl. Phys. Lett.* **74**, 317 (1999).
 - [20] V. L. Colvin, M. C. Schlamp, and A. P. Alivisatos, *Nature (London)* **370**, 354 (1994).
 - [21] M. C. Schlamp, X. Peng, and A. P. Alivisatos, *J. Appl. Phys.* **82**, 5837 (1997).
 - [22] N. C. Greenham, X. Peng, and A. P. Alivisatos, *Phys. Rev. B* **54**, 17 628 (1996).
 - [23] L. W. Wang and A. Zunger, *Phys. Rev. B* **53**, 9579 (1996).